Steady-state cooperative effects in a continuously generating superradiant Raman laser

© *K. S. Tikhonov*[1]*, A. Roth*[2]

[1] St. Petersburg State University,
199034 St. Petersburg, Russia,
[2] Leibniz University Hannover,
30167, Hannover, Germany

e-mail: tikhonov.kyril@gmail.com

A generalized model of the continuously generating superradiant Raman laser is considered. The model includes competing individual and cooperative atomic processes arising from the interaction of atoms with external light fields. We show that proper selection of the model parameters leads to cooperative effects in the atomic active laser medium. We calculate the steady state values of the atomic polarization and two-atom correlations. Using the quantum regression theorem, we determine the spectral characteristics of the collectively emitted light. We use cumulant expansion to estimate the higher-order correlations between atoms.

Keywords: superradiant laser, correlated states of atoms, cooperative effects, cumulant expansion.

1. Introduction

The operation of a superradiant laser [1] is based on the phenomenon of cooperative spontaneous emission (or the Dicke superradiance) [2]. Unlike conventional lasers, whose active medium is located in a high-quality, „good" cavity, the superradiant laser operates in the regime of the so-called „bad" cavity [3]. In such a regime the photons of the generated light leave the cavity almost instantly, but this turns out to be sufficient to match the phases of individual emitting atoms with each other, which leads to the formation of a long-lived collective coherence in the atomic medium. Over time, correlations between atoms accumulate and along the cavity axis the ensemble of atoms radiates as a whole with a radiation line width comparable to the width of the atomic laser transition. In theory, the superradiant laser operating on a clock transition can achieve a radiation line width about 1 mHz [4]. Since the coherence of the emitted light is determined by the atomic medium, not by the cavity, the superradiant laser is almost insensitive to both thermal and technical vibrations of mirrors, which impose a fundamental stability limitation for laser sources with passive optical cavities [5,6]. Thus, due to the high stability and narrowness of the spectral line, the superradiant lasers are often considered in the context of a new generation of atomic clocks and frequency standards [7]. However, this does not mean at all that the superradiant sources of coherent radiation are not in demand in other areas. In particular, amplification of spontaneous radiation due to the effect of superradiance can also occur at two-photon Raman transitions, which has already been shown in experimental works [8,9]. Such radiation sources are of interest for a number of important problems of magnetometry [10], as well as for generating nonclassical states of light [11].

The simplest model of a superradiant laser, which describes the dynamics of a two-level atomic system in the presence of external electromagnetic fields, includes the individual pumping of atoms from the ground state to the excited state and their collective decay in the reverse transition [4,12]. In this paper, we will consider a generalized model of a superradiant Raman laser, which (in addition to individual pumping and decay of atoms) includes two competing cooperative processes acting on the transition between the ground and excited states of the effective two-level scheme. Such processes are characteristic of atoms with a complex multilevel energy structure, such as Rubidium and Cesium, which are usually used in optical experiments. Note that even in the case of a simple model of the superradiant laser, the cooperative generation occurs only for a certain choice of its parameters. In particular, the rate of individual pumping of atoms by an external laser field must exceed the decay rate of the excited state of the atom in order to create a population inversion in the atomic medium, but at the same time it should not be too high so as not to destroy the phase correlations that arise between individual emitters. In the generalized model under consideration, due to the presence of several competing processes the balance between the parameters takes on a much more complex form. In this paper we will find the range of values of the model parameters at which the cooperative radiation of the atomic medium occurs, and determine the spectral characteristics of light at the output of the cavity in the stationary state.

The paper is organized as follows. In Section 2 we will consider the simplest model of the superradiant laser, with the help of which we will describe its most important characteristics in the stationary state. In particular, we

will be interested in the average polarization of atoms (population inversion of the atomic medium) and two-atom correlations, the presence of which, as we shall see, will indicate the occurrence of cooperative effects in the medium. The results obtained will help in the analysis of solutions for the generalized model of the superradiant laser in Section 3, in which we will find the radiation spectrum and determine its characteristics. In particular, we will show that, under optimal generation conditions, the width of the spectral line of the radiation will be comparable to the width of the atomic transition. In Section 4 using the cumulant expansion we will estimate the presence of higher-order correlations between atoms in the stationary state of generation of the superradiant laser. Besides, in this paper we will pay special attention to a number of theoretical methods that are often used in the study of the superradiant laser: the quantum regression theorem, yielding the radiation spectrum, and cumulant analysis, which will allow us to determine the presence of interatomic correlations in the system.

2. Superradiant laser model

First, let us consider the simplest model of the super-radiant laser, which defines to describe the main physical processes occurring in it, leading to cooperative emission of atoms. Its general view is schematically shown in Fig. 1, a. An ensemble of N two-level atoms is placed inside a single-mode cavity with line width κ. The cavity is chosen so that the frequency ω_c of the $\hat{a}$ mode, supported by it, coincides with the frequency ω_{eg} of the transition between the ground $|g\rangle$ and the excited $|e\rangle$ levels of the atom, i.e. $\omega_c = \omega_{eg}$. We describe the interaction between the cavity field and atoms using the dipole approximation, while assuming that the field interacts with each atom in the same way, and the interaction strength is determined by the single-photon Rabi frequency $\Omega/2$ (Fig. 1, b). The time evolution of the state of the system obeys the Lindblad master equation:

$$\frac{d}{dt}\rho = -i\frac{\omega_{eg}}{2}[J^z + \hat{a}^\dagger\hat{a}, \rho] - i\frac{\Omega}{2}[J^+\hat{a} + J^-\hat{a}^\dagger, \rho]$$

$$+ w\sum_i \mathscr{D}[\sigma_i^+]\rho + \kappa\mathscr{D}[\hat{a}]\rho, \qquad (1)$$

where using $\mathscr{D}[A]\rho = A\rho A^\dagger - 1/2A^\dagger A\rho - 1/2\rho A^\dagger A$ the Lindblad superoperators are designated, $J^z = \sum_{i=1}^{N}\sigma_i^z$ and $J^\pm = \sum_{i=1}^{N}\sigma_i^\pm$ are collective angular momentum operators written in terms of the Pauli matrix σ_i^z and ladder (raising and lowering) operators of the $\sigma_i^\pm$ of ith atom. Besides the coherent interaction of the atoms with the intracavity field, we also included in equation (1) the photons escape from the cavity with the rate κ, and the individual pumping of the atoms with the rate w, which transfers the atoms from the ground state $|g\rangle$ to the excited state $|e\rangle$. Note that the individual nature of pumping is important due to two reasons. First, as was shown in papers [12,13], only in this

case the collective dipole moment of the atoms ensemble is formed, i.e. the ensemble radiates as a whole. Second, individual pumping can balance other incoherent processes, such as individual spontaneous decay of atoms. For the simplicity of analysis, individual spontaneous decay was not included in equation (1), but its contribution will be evaluated later when considering the generalized model of the superradiant laser in Section 3.

Unlike conventional lasers, whose radiation coherence depends on the properties of the cavity, the radiation coherence of the superradiant laser is determined by cooperative effects in the atomic medium. These effects arise in the bad cavity regime, when the photons escape from the cavity is faster than other processes in (1), i.e. $\kappa \gg w, \Omega$. This makes it possible to adiabatically eliminate the field $\hat{a}$ from the Lindblad equation and consider the dynamics of the atomic state separately [12]. To do this, we used the projector method described in [14]. As a result, after the adiabatic elimination of the cavity mode, a master equation was obtained describing the evolution of the density matrix ρ_{at} of the atomic system:

$$\frac{d}{dt}\rho_{at} = w\sum_i \mathscr{D}[\sigma_i^+]\rho_{at} + \gamma\mathscr{D}[J^-]\rho_{at}, \qquad (2)$$

where $\gamma = \Omega^2/\kappa$ is the effective decay rate of atom from excited state $|e\rangle$ to the ground state $|g\rangle$.

From (2) we derive a system of equations describing the time evolution of the mean values for the polarization (population inversion) $\langle\sigma_1^z\rangle$ and two-atom correlations $\langle\sigma_1^+\sigma_2^-\rangle$ containing the relative phase between two emitters:

$$\frac{d}{dt}\langle\sigma_1^z\rangle = w(1 - \langle\sigma_1^z\rangle) - \gamma(1 + \langle\sigma_1^z\rangle)$$

$$- 2(N-1)\gamma\langle\sigma_1^+\sigma_2^-\rangle,$$

$$\frac{d}{dt}\langle\sigma_1^+\sigma_2^-\rangle = \{(N-2)\gamma\langle\sigma_1^z\rangle - (w+\gamma)\}\langle\sigma_1^+\sigma_2^-\rangle$$

$$+ \frac{\gamma}{2}(\langle\sigma_1^z\rangle + 1)\langle\sigma_1^z\rangle. \qquad (3)$$

Subscript denotes the number of the atom. Due to permutation symmetry, each atom of the ensemble interacts with the cavity mode and external pumping in the same way. Thus, the 1st and the 2nd atom can be chosen in an arbitrary way. Besides, when writing the system of equations (3) we used the cumulant expansion, in which we neglected third-order correlations and factorized the moment $\langle\sigma_1^+\sigma_2^-\sigma_3^z\rangle = \langle\sigma_1^+\sigma_2^-\rangle\langle\sigma_3^z\rangle$, and also approximate $\langle\sigma_1^z\rangle\langle\sigma_2^z\rangle = \langle\sigma_1^z\rangle^2$ [15]. The presence of higher-order correlations will be estimated in Section 4.

To find the average values of polarization $\langle\sigma_1^z\rangle$ and two-atom correlations $\langle\sigma_1^+\sigma_2^-\rangle$ established in the stationary state of superradiant laser generation, it is necessary to equate the left part (3) to zero, and then solve the resulting homogeneous system of equations. Fig. 2 shows the dependences of these observations on the dimensionless individual pumping rate of atoms $w/N\gamma$. It can be seen
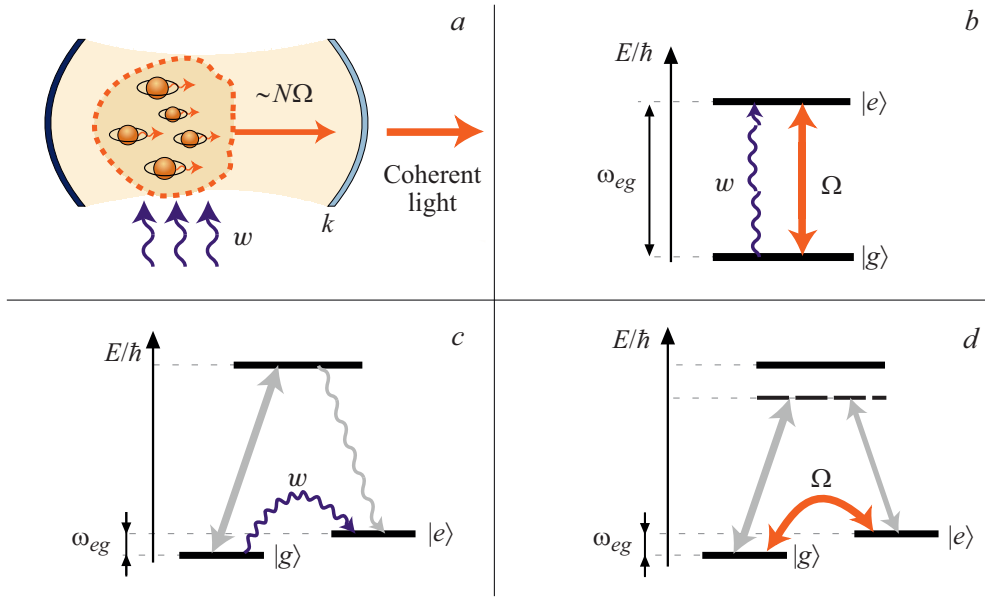
Figure 1. (a) Superradiant laser based on an ensemble of N atoms placed in the cavity with line width κ; (b) the effective two-level energy scheme of atoms inside cavity, which in practice can be implemented through the processes shown in (c) and (d). w — effective pumping rate of atoms, $\Omega/2$ — effective single-photon Rabi frequency, (c) optical pumping of atom with λ-scheme of levels, (d) two-photon Raman transition induced by external field in atom with λ-scheme of levels.
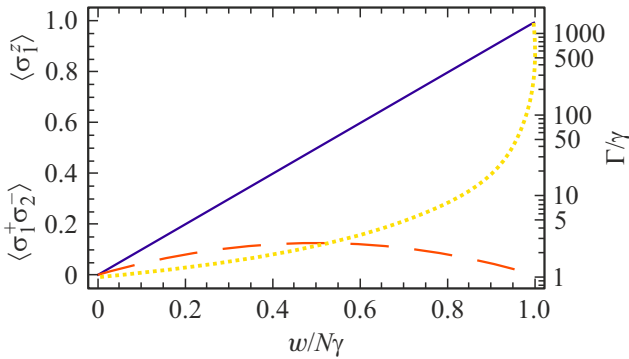

Figure 2. Average polarization $\langle \sigma_1^z \rangle$ (dark purple solid line), two-atom correlations $\langle \sigma_1^+ \sigma_2^- \rangle$ (orange dashed line) and the spectral line width Γ, expressed in units of the effective decay rate of the atom γ from the excited state $|e\rangle$ to the ground state $|g\rangle$ (yellow dotted line) in the stationary state of superradiant laser generation. Number of atoms $N = 10^6$.

from the figure that the polarization increases linearly as the pumping rate increases, while the curve for two-atom correlations describes an inverted parabola that grows from zero at $w/N\gamma = 0$ to a maximum value at $w/N\gamma = 0.5$, and then decreasing to zero at $w/N\gamma = 1$. The presence of nonzero values of two-atom correlations, indicates the occurrence of superradiance, at which the rate of the atom transition γ from the excited state $|e\rangle$ to the ground state $|g\rangle$ is enhanced depending on the number of atoms in the excited state. It can be seen from the graphs that, for this case the pumping rate of atoms w must satisfy the following

boundary conditions:

$$\gamma < w < N\gamma. \qquad (4)$$

Here, the lower boundary $w_{\min} = \gamma$ corresponds to the appearance of the population inversion in the atomic medium, which is necessary for laser generation. This differs significantly from the conventional laser, in which the lower generation threshold is reached when the pumping exceeds the cavity losses. The upper boundary $w_{\max} = N\gamma$ corresponds to the situation when the cooperative emission of atoms disappears due to the presence of noise caused by the pumping itself.

To calculate the radiation spectrum, we used the quantum regression theorem (Section 3), and found that its value is determined by the Fourier transformation taken from the two-time correlation function of collective atomic operators:

$$S(\omega) = \mathscr{F}[\langle \hat{a}^\dagger(t)\hat{a}(0) \rangle](\omega) = \frac{\Omega^2}{\kappa^2} \mathscr{F}[\langle J^+(t)J^-(0) \rangle](\omega), \qquad (5)$$

which in turn can be determined from the equation assuming stationary state

$$\frac{d}{dt}\langle J^+(t)J^-(0) \rangle = \left(i\omega_{eg} - \frac{\Gamma}{2} \right) \langle J^+(t)J^-(0) \rangle. \qquad (6)$$

As we will see below, the radiation spectrum has a Lorentz profile with the line width $\Gamma = w + \gamma - (N-1)\gamma \langle \sigma_1^z \rangle$, which, with the optimal choice of pumping rate w corresponding to the maximum of two-atom correlations $\langle \sigma_1^+ \sigma_2^- \rangle$ turns out to be comparable with γ (Fig. 2).

The above model of the superradiant laser is based on the use of an ensemble of two-level atoms, and, as was shown in the papers [4,12], it is sufficient to describe the main properties of the resulting cooperative radiation. In practice, this model can be implemented, in particular, with the help of two-photon Raman transitions induced by external fields in atoms with λ-configuration of energy levels (Fig. 1, c, d). In this case, due to the presence of a detuning from resonance, the upper level can be adiabatically eliminated; i.e. atoms can be described with the effective two-level scheme. However, in actual atoms with complex energy structure of levels, the nonresonant two-photon Raman transitions lead to the additional cooperative and individual terms in the equation for the density matrix. These terms compete with each other resulting in new conditions for the appearance of the superradiant laser transition in the medium (or even several such transitions).

3. Generalized model of superradiant Raman laser

3.1. Master equation

As was shown in the previous section, even in a simplified model the superradiance requires maintaining a certain balance between the individual pumping rate and the cooperative decay rate. In this section we consider a generalized model of the superradiant Raman laser, which includes additional competing cooperative and individual processes arising in the effective two-level scheme of atoms due to nonresonant two-photon Raman transitions (Fig. 3). These additional processes lead to the occurrence of a new, finer balance between the model parameters, which is necessary for the superradiance.

The dynamics of the state of the atomic-field system under consideration after the adiabatic elimination of nonresonant energy levels is described by the following master equation, obtained with the rotating frame approximation [16]:

$$\frac{d}{dt}\rho = -i\frac{\omega_{eg}}{2}\Big[J^z,\rho\Big] - i\Big[\Big(\frac{\Omega_-}{2}J^+ + \frac{\Omega_+}{2}J^-\Big)\hat{a} + h.c., \rho\Big]$$
$$+ w_+\sum_i \mathscr{D}\big[\sigma_i^+\big]\rho + w_-\sum_i \mathscr{D}\big[\sigma_i^-\big]\rho + \kappa\mathscr{D}\big[\hat{a}\big]\rho,$$

$$(7)$$

where ω_{eg} is frequency difference between two sublevels of the ground state of the atom $|g\rangle$ and $|e\rangle$. In accordance with the Jaynes-Cummings model, this equation includes a cooperative term proportional to the effective Rabi frequency Ω_-, which describes the transition of the atoms from the level $|g\rangle$ to the level $|e\rangle$ as a result of interaction with the cavity mode $\hat{a}$ and an external classical field (in Fig. 3, a is shown by the left straight vertical arrow), as well as a cooperative term proportional to the effective frequency Ω_+ acting on the reverse transition, i.e. from the level $|e\rangle$ to the level $|g\rangle$, and induced by another classical
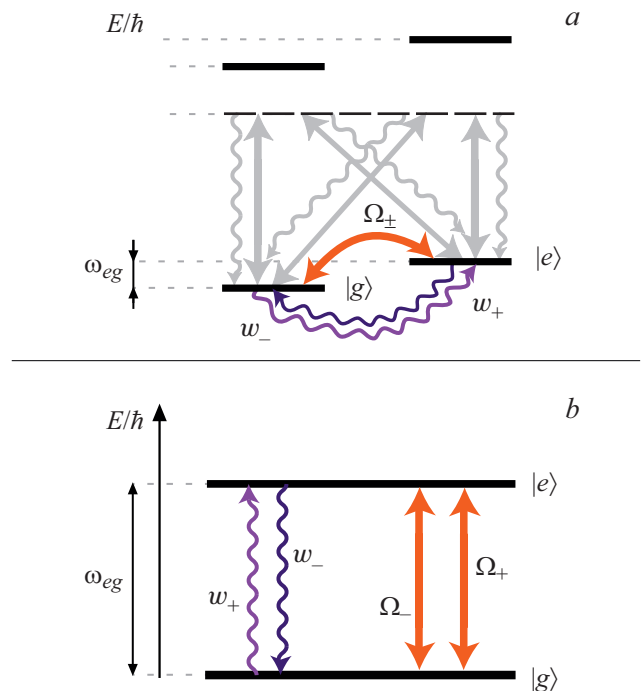

Figure 3. (*a*) The energy scheme of atomic levels, which designates the processes of individual pumping with an effective rate w_+ on the transition $|g\rangle \to |e\rangle$, of individual pumping with an effective rate w_- on the $|e\rangle \to |g\rangle$ transition, as well as two-photon Raman transitions induced by external fields, occurring at an effective one-photon Rabi frequency $\Omega/2$; (*b*) The simplified effective scheme of atomic levels, which includes only the processes that are relevant for the considered system.

field (in Fig. 3, a is shown by the right straight vertical arrow). Note that if the energy gap ω_{eg} between the levels is small compared to the frequency of external classical fields, then they act the both transitions (Fig. 3, a). Besides, we also included in the model the individual pumping process with an effective rate w_+ on the transition $|g\rangle \to |e\rangle$ and individual pumping process with an effective rate w_- acting on the transition $|e\rangle \to |g\rangle$, as well as the photons escape from the cavity with the rate κ.

As before, we assume that the photons escape from the cavity is much faster than all other processes included in (7), i.e., $\kappa \gg \Omega_\pm, w_\pm$. After the adiabatic elimination of the cavity field using the projectors method, we obtain the master equation for the density matrix, which describes the time evolution of the atomic system only:

$$\frac{d}{dt}\rho_{at} = -i\frac{\omega_{eg}}{2}\Big[J^z,\rho_{at}\Big] + w_+\sum_i \mathscr{D}\big[\sigma_i^+\big]\rho_{at}$$
$$+ \gamma_-\mathscr{D}\big[J^-\big]\rho_{at} + w_-\sum_i \mathscr{D}\big[\sigma_i^-\big]\rho_{at} + \gamma_+\mathscr{D}\big[J^+\big]\rho_{at},$$

$$(8)$$

where $\gamma_- = \Omega_-^2/\kappa$ is the effective decay rate of atom from the excited state $|e\rangle$ to the ground state $|g\rangle$, and $\gamma_+ = \Omega_+^2/\kappa$ is the effective rate of the backward transition.

In the resulting equation the second and the third terms corresponding to individual pumping at the $|g\rangle \to |e\rangle$ transition and cooperative decay at the $|e\rangle \to |g\rangle$ transition coincide with the right side of equation (2). At the same time, the fourth and the fifth terms represent individual „pumping" and cooperative „decay" in the opposite direction, i.e. act as if the symbols of levels $|e\rangle$ and $|g\rangle$ were reversed. Thus, a certain symmetry arises in the resulting equation: if we replace „pluses" with „minuses" and „minuses" with „pluses", then the form of the equation does not change. This symmetry is convenient for use in the analysis of the obtained solutions. In particular, without loss of generality, it is sufficient to consider only those cases where $w_+ > w_-$. As follows from the solutions for the simplified model shown in Fig. 2, the cooperative effects in atomic medium appear when a sufficient populations inversion is created in the medium, at which the individual pumping rate w is comparable in order of magnitude to the cooperative decay rate $N\gamma$. Thus, we are interested in the area $w_+, w_- \gg \gamma_-, \gamma_+$. Without loss of generality, we assume $\gamma_- > \gamma_+$. In all other cases, the system behaves in a similar way, with the only difference that the atomic levels are „swapped".

From (8) it is easy to derive equations for polarization $\langle \sigma_1^z \rangle$ and two-atom correlations $\langle \sigma_1^+ \sigma_2^- \rangle$:

$$\frac{d}{dt}\langle \sigma_1^z \rangle = w_+(1 - \langle \sigma_1^z \rangle) - w_-(1 + \langle \sigma_1^z \rangle)$$
$$- 2(N-1)(\gamma_- - \gamma_+)\langle \sigma_1^+ \sigma_2^- \rangle,$$

$$\frac{d}{dt}\langle \sigma_1^+ \sigma_2^- \rangle = \{(N-2)(\gamma_- - \gamma_+)\langle \sigma_1^z \rangle$$
$$- (w_+ + w_- + \gamma_- + \gamma_+)\}\langle \sigma_1^+ \sigma_2^- \rangle$$
$$+ \frac{1}{2}((\gamma_- - \gamma_+) + (\gamma_- + \gamma_+)\langle \sigma_1^z \rangle])\langle \sigma_1^z \rangle,$$
(9)

where, as earlier, the third-order correlations were neglected, and the following moments were factorized [15]: $\langle \sigma_1^z \sigma_2^z \rangle \approx \langle \sigma_1^z \rangle^2$ and $\langle \sigma_1^+ \sigma_2^- \sigma_3^z \rangle \approx \langle \sigma_1^+ \sigma_2^- \rangle \langle \sigma_1^z \rangle$. To find a stationary solution to these equations, one must set the left hand side of the equations equal to zero and then solve the resulting linear system.

Fig. 4, a shows the solutions of stationary equations for the mean polarization $\langle \sigma_1^z \rangle$ and two-atomic correlations $\langle \sigma_1^+ \sigma_2^- \rangle$ depending on the dimensionless pumping rate $w_+/N\gamma_-$, normalized to the number of atoms N, at $\gamma_+ = 0$, i.e. in the presence of only one cooperative decay in (8) from the level $|e\rangle$ to the level $|g\rangle$. The solid curves correspond to simplified model of the superradiant laser with $w_- = 0$ (as in Fig. 2), which we use for comparison. The dashed and dotted lines correspond to the other two cases, when $w_-/N\gamma_- = 0.03$ and $w_-/N\gamma_- = 0.06$. It can be seen that the presence of additional individual term in (8) on the transition from $|e\rangle \to |g\rangle$ (it can be considered as an individual decay) leads to the shift in the lower and
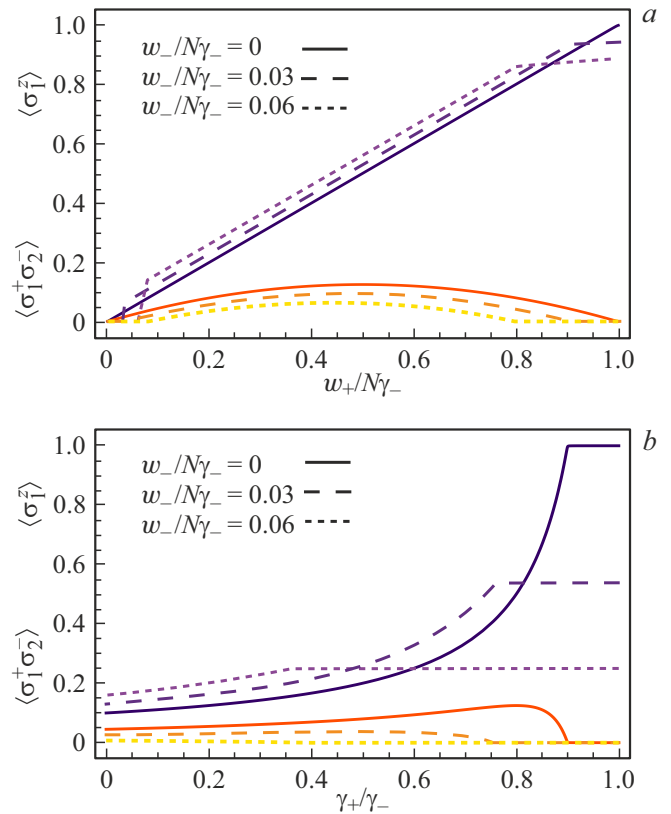

Figure 4. Mean polarization $\langle \sigma_1^z \rangle$ (three upper lines), two-atom correlations $\langle \sigma_1^+ \sigma_2^- \rangle$ (three lower lines) depending on the following parameters of the problem: (a) dimensionless pumping $w_+/N\gamma_-$ on the transition $|g\rangle \to |e\rangle$; (b) dimensionless rate of the cooperative process γ_+/γ_- on the transition $|g\rangle \to |e\rangle$. Number of atoms $N = 10^6$.

upper generation thresholds, i.e. changing the boundary conditions (4). In this case, the polarization of the medium rises with the pumping rate w_+ up to a certain value, after which it reaches saturation. Maximum of two-atom correlations

$$\max_{w_+} \langle \sigma_1^+ \sigma_2^- \rangle = \frac{1}{8} - \frac{w_-}{N\gamma_+} \frac{1}{\frac{\gamma_-}{\gamma_+} - 1}$$

is achieved at the pumping rate $w_{+,\text{opt}} = N(\gamma_- - \gamma_+)/2 - w_-$ for $N \gg 1$.

Fig. 4, b shows the mean polarization $\langle \sigma_1^z \rangle$ and the two-atom correlations $\langle \sigma_1^+ \sigma_2^- \rangle$ vs. γ_+/γ_- for $w_+/N\gamma_- = 0.1$. It can be seen that two-atom correlations in the system turn out to be very sensitive to the presence of individual decay of atoms from the level $|e\rangle$ to the level $|g\rangle$.

The stationary solution for the two-atom correlations $\langle \sigma_1^+ \sigma_2^- \rangle$ demonstrates that superradiance occurs in the system when the individual pumping rate w_+ satisfies the following inequalities:

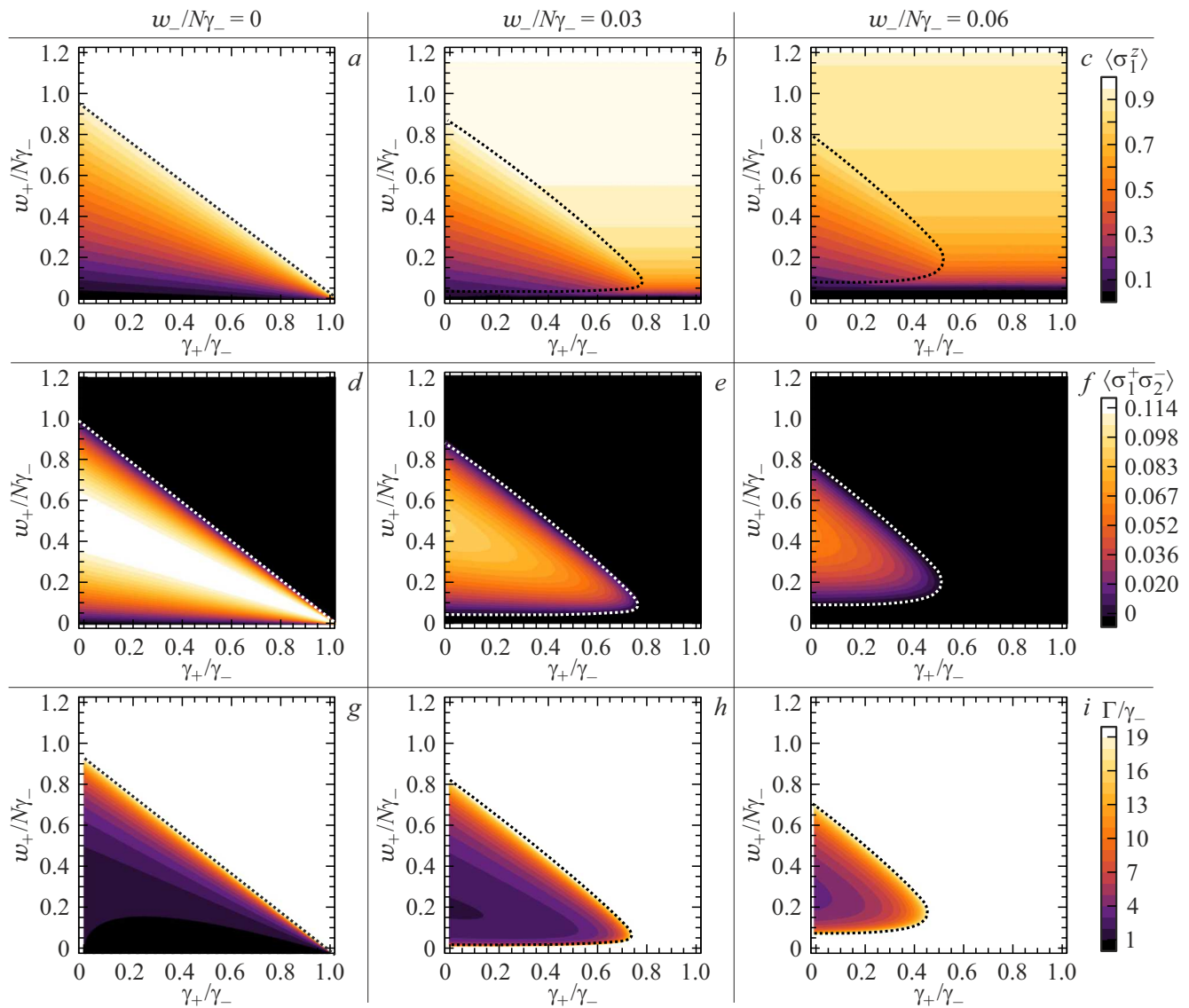$$w_- < w_+ < N(\gamma_- - \gamma_+)\frac{w_+ - w_-}{w_+ + w_-} - w_-. \quad (10)$$

Figure 5. (*a–c*) Polarization $\langle \sigma_1^z \rangle$; (*d–f*) of two-atom correlations $\langle \sigma_1^+ \sigma_2^- \rangle$; (*g–i*) dimensionless width of spectral line Γ / γ_- as a function of the dimensionless individual pumping rate $w_\pm / N\gamma_-$, normalized to the number of atoms N, and dimensionless velocity γ_+ / γ_-. Number of atoms $N = 10^6$.

Compared to the previously obtained boundary conditions (4) for simplified model of the superradiant laser, the new boundary conditions depend on all four rates included in (8). Thus, a finer balance between them is required for the cooperative generation of coherent light.

Fig. 5, *a–f* shows the general view of the mean polarization $\langle \sigma_1^z \rangle$ and two-atom correlations $\langle \sigma_1^+ \sigma_2^- \rangle$ vs. dimensionless individual pumping rate $w_+ / N\gamma_-$, normalized to the number of atoms N, and the dimensionless rate γ_+ / γ_- of the cooperative process on transition $|g\rangle \rightarrow |e\rangle$. In Fig. 5, *a–f* (as well as Fig. 5, *g–i*), the dotted curve designates the range of parameter values at which cooperative radiation occurs in the atomic medium, which is confirmed by the spectrum calculation.

3.2. Radiation spectrum

To find the radiation spectrum generated by the superradiant Raman laser, we apply the quantum regression theorem [14,17]. For this purpose, let us return to master equation (7), which describes the time evolution of the density matrix of the system before the adiabatic elimination of the cavity. With its help we derive the equation for the mean value of the annihilation operator $\hat{a}$:

$$\frac{d}{dt} \langle \hat{a}(t) \rangle = -\frac{\kappa}{2} \langle \hat{a}(t) \rangle - i \left(\Omega_+ \langle J^-(t) \rangle + \Omega_- \langle J^+(t) \rangle \right). \tag{11}$$

The right-hand side of the equation includes the mean values of the atomic collective raising and lowering operators $\langle J^+(t) \rangle$ and $\langle J^-(t) \rangle$. Since $\kappa \gg w_\pm, \Omega_\pm$, the change

over time $\langle J^+(t)\rangle$ and $\langle J^-(t)\rangle$ is slower than $\langle \hat{a}(t)\rangle$, which makes it possible to use the master equation for the density matrix of atomic system (8) to determine their time evolution instead of the equation for the density matrix of the complete system (7). We get the following equations:

$$\frac{d}{dt}\langle J^-(t)\rangle = -iw_{eg}\langle J^-(t)\rangle$$
$$-\frac{1}{2}\{\gamma_- + \gamma_+ + \omega_+ + \omega_- - (\gamma_- - \gamma_+)N\langle\sigma_1^z\rangle\}\langle J^-(t)\rangle, \quad (12)$$

$$\frac{d}{dt}\langle J^+(t)\rangle = +iw_{eg}\langle J^+(t)\rangle$$
$$-\frac{1}{2}\{\gamma_- + \gamma_+ + \omega_+ + \omega_- - (\gamma_- - \gamma_+)N\langle\sigma_1^z\rangle\}\langle J^+(t)\rangle, \quad (13)$$

solving which, we find:

$$\langle J^-(t)\rangle = \langle J^-(0)\rangle e^{-\frac{1}{2}\Gamma t}e^{-iw_{eg}t}, \quad (14)$$

$$\langle J^+(t)\rangle = \langle J^+(0)\rangle e^{-\frac{1}{2}\Gamma t}e^{+iw_{eg}t}, \quad (15)$$

where $\Gamma = \gamma_- + \gamma_+ + \omega_+ + \omega_- - (\gamma_- - \gamma_+)N\langle\sigma_1^z\rangle$ is the linewidth of the spectrum. Substituting the obtained solutions for $\langle J^+(t)\rangle$ and $\langle J^-(t)\rangle$ into (11), we get the following inhomogeneous differential equation:

$$\frac{d}{dt}\langle \hat{a}(t)\rangle + \frac{\kappa}{2}\langle \hat{a}(t)\rangle = -i\left(\Omega_+\langle J^-(0)\rangle e^{-\frac{1}{2}\Gamma t}e^{-iw_{eg}t}\right.$$
$$\left. + \Omega_-\langle J^+(0)\rangle e^{-\frac{1}{2}\Gamma t}e^{iw_{eg}t}\right), \quad (16)$$

from which we find:

$$\langle \hat{a}(t)\rangle = C(0)e^{-\frac{\kappa t}{2}} + i\left(\frac{\Omega_-\langle J^+(0)\rangle}{-iw_{eg} + (\Gamma - \kappa)/2}e^{iw_{eg}t}\right.$$
$$\left. + \frac{\Omega_+\langle J^-(0)\rangle}{iw_{eg} + (\Gamma - \kappa)/2}e^{-iw_{eg}t}\right)e^{-\Gamma t/2}, \quad (17)$$

where $C(0) = 0$, since there is no field at the initial time.

According to the quantum regression theorem [14,17], for a set of operators $\{Y_i\}$ of open quantum system whose mean values are described by a closed linear system of differential equations

$$\partial_t\langle Y_i(t)\rangle = \sum_j G_{ij}(t)\langle Y_j(t)\rangle,$$

where $G_{ij}(t)$ are some functions relating these mean values to each other, the two-time correlation function can be written as

$$\partial_t\langle Y_i(t+\tau)Y_k(t)\rangle = \sum_j G_{ij}(\tau)\langle Y_j(t+\tau)Y_k(t)\rangle.$$

Thus, from (17) it follows the expression for the two-time correlation function $\langle \hat{a}^\dagger(t)\hat{a}(0)\rangle$:

$$\langle \hat{a}^\dagger(t)\hat{a}(0)\rangle = \left(\frac{\Omega_-^2\langle J^-(0)J^+(0)\rangle}{w_{eg}^2 + (\Gamma - \kappa)^2/4}e^{-iw_{eg}t}\right.$$
$$\left. + \frac{\Omega_+^2\langle J^+(0)J^-(0)\rangle}{w_{eg}^2 + (\Gamma - \kappa)^2/4}e^{iw_{eg}t}\right)e^{-\Gamma t/2}. \quad (18)$$
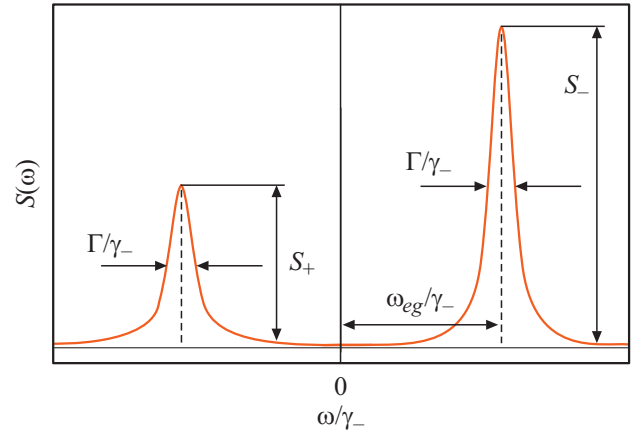

Figure 6. The form of the radiation spectrum $S(\omega)$ and its characteristics.

The radiation spectrum follows from the Fourier transformation:

$$S(\omega) = \mathscr{F}[\langle \hat{a}^\dagger(t)\hat{a}(0)\rangle](\omega).$$

It can be seen that the presence of the two cooperative transitions of atoms $|e\rangle \to |g\rangle$ and $|g\rangle \to |e\rangle$ on the right-hand side (7) leads to two Lorentz peaks. In this case, the spectral width Γ for each of them is the same (for $w_+ > w_-$ and $N \gg 1$) and equal to

$$\frac{\Gamma}{\gamma_-} \approx \left(\frac{1}{W_-(1-W_+)} + \frac{W_+}{1-W_+} - W_+ - \frac{1}{W_-}\right)\left(1 - \frac{\gamma_+}{\gamma_-}\right)$$

$$= \frac{W_+ + W_+W_-(W_- - W_+W_- - 1)}{(W_+ - 1)(W_- - 1)W_-}\left(1 - \frac{\gamma_+}{\gamma_-}\right), \quad (19)$$

where, for convenience, we introduced the dimensionless value

$$W_\pm := \frac{(w_+ \pm w_-)(w_+ + w_-)}{N(\gamma_- - \gamma_+)(w_+ - w_-)}.$$

Fig. 5, g–i shows the dimensionless line width Γ/γ_- as a function of the same parameters of the generalized model as for the previously analyzed mean polarizations and two-atom correlations. It can be seen that, as for the simplified model of the superradiant laser, the linewidth in the generalized case also turns out to be comparable to γ_- in the region where nonzero two-atom correlations exist, and the boundary conditions (10) are satisfied. For clarity, Fig. 6 schematically shows the form of the resulting radiation spectrum, where S_+ and S_- designate the intensities of the Lorentz peaks. Moreover, their relationship obeys

$$\frac{S_+}{S_-} = \frac{\gamma_+}{\gamma_-}\frac{1}{1 - \frac{\langle J^z\rangle}{\langle J^+J^-\rangle}} \approx \frac{\gamma_+}{\gamma_-}. \quad (20)$$

Note that the peak intensities cannot be the same, since the boundary conditions (10) are not satisfied at $\gamma_+ = \gamma_-$.

4. Influence of high-order correlations

In this section, we estimate the presence of high-order interatomic correlations in the stationary state. For simplicity, we analyze the simplified model described by equation (2), when there are only the cooperative transition on the $|e\rangle \rightarrow |g\rangle$ transition and the individual pumping on the $|g\rangle \rightarrow |e\rangle$ transition. Let us write the master equation for the reduced density matrix of a subensemble of n arbitrarily taken atoms (the subscript „at", which was used earlier to designate the atomic system, will be omitted here and below):

$$\dot{\rho}_n = L_n(\rho_n)$$
$$- \frac{1}{2}\gamma(N-n)\sum_{i=1}^{n}\left\{\sigma_-^{(i)}\operatorname{Tr}_{\{n+1\}}[\sigma_+^{(n+1)}\rho_{n+1}] + h.c.\right\},$$
$$(21)$$

where $\rho_n = \operatorname{Tr}_{\{n+1,\ldots,N\}}[\rho]$ is the reduced density matrix for n particles. Curved brackets indicate tracing out of remaining $(N-n)$ particles. On the right-hand side of the equation, L_n designates the superoperator that performs the time evolution of ρ_n according to (2). Here, we took into account that the atoms interaction with the intracavity field is the same, and the ensemble turns out to be symmetrical with respect to the permutation of any two particles. Thus one can describe the interactions of the considered subensemble with the remaining $(N-n)$ atoms with the reduced density matrix ρ_{n+1} of n particles of the subensemble and one of the remaining $(N-n)$.

Equation (21) turns out to be non-closed, since its right-hand side contains the reduced density matrix ρ_{n+1}, which describes the state of $(n+1)$ particles. To remove $(n+1)$-order correlations from the system and to express ρ_{n+1} in terms of ρ_n, we apply the cumulant expansion. The convenience of cumulants lies in the fact that, unlike moments the nonzero cumulant of the n-th order shows the presence of correlations between n parts at once, i.e. it does not include lower-order correlations of it parts.

It is well known that the moments are the coefficients of the expansion in series of the characteristic function, while the cumulants are the coefficients of the expansion of its logarithm [18]. There is a bijective map between cumulants and moments [19]. So, for example, for cumulants and moments from the 1st order to the 3rd order, we have:

$$\langle\langle \sigma_1^{\alpha_1}\rangle\rangle = \langle \sigma_1^{\alpha_1}\rangle,$$

$$\langle\langle \sigma_1^{\alpha_1}\sigma_2^{\alpha_2}\rangle\rangle = \langle \sigma_1^{\alpha_1}\sigma_2^{\alpha_2}\rangle - \langle \sigma_1^{\alpha_1}\rangle\langle \sigma_2^{\alpha_2}\rangle,$$

$$\langle\langle \sigma_1^{\alpha_1}\sigma_2^{\alpha_2}\sigma_3^{\alpha_3}\rangle\rangle = \langle \sigma_1^{\alpha_1}\sigma_2^{\alpha_2}\sigma_3^{\alpha_3}\rangle - \langle \sigma_1^{\alpha_1}\sigma_2^{\alpha_2}\rangle\langle \sigma_3^{\alpha_3}\rangle$$
$$- \langle \sigma_1^{\alpha_1}\sigma_3^{\alpha_3}\rangle\langle \sigma_2^{\alpha_2}\rangle - \langle \sigma_2^{\alpha_2}\sigma_3^{\alpha_3}\rangle\langle \sigma_1^{\alpha_1}\rangle$$
$$+ 2\langle \sigma_1^{\alpha_1}\rangle\langle \sigma_2^{\alpha_2}\rangle\langle \sigma_3^{\alpha_3}\rangle.$$
$$(22)$$

Here $\sigma_i^{\alpha_i}$ is the operator acting on the state of the i-th atom. The superscript α_i, as before, specifies a specific type of the operator (for example, „z", „+", „−"). Cumulants

are designated by double angle brackets, and moments by single angle brackets. The general expression connecting cumulants and moments of an arbitrary order can be written as follows:

$$\left\langle\left\langle \bigotimes_{i\in\mathbb{A}}\sigma_i^{\alpha_i}\right\rangle\right\rangle = \sum_{\pi\in\pi_{\mathbb{A}}}(|\pi|-1)!(-1)^{|\pi|-1}\prod_{\mathbb{B}\in\pi}\left\langle\bigotimes_{i\in\mathbb{B}}\sigma_i^{\alpha_i}\right\rangle,$$
$$(23)$$

where $\mathbb{A}$ is some set of particle numbers, which is a subset of $\{1,\ldots,N\}$, i.e. $\mathbb{A}\subseteq\{1,\ldots,N\}$. $|\pi|$ denotes the number of elements of π set, and $\pi_{\mathbb{A}}$ is the set of all possible partitions of the set $\mathbb{A}$. For example, for $\mathbb{A}=\{1,2,3\}$ the set $\pi_{\mathbb{A}}$ consists of the next partitions $\{1,2,3\}$: $\{\{1,2\},\{3\}\}$, $\{\{1\},\{2,3\}\}$, $\{\{1,3\},\{2\}\}$, $\{\{1\},\{2\},\{3\}\}$.

In quantum mechanics, the moments can be calculated not only through the characteristic function, but also directly, taking the trace from the product of the corresponding operators and the density matrix describing the state of the system, i.e. $\langle\otimes_{i\in\mathbb{A}}A_i^{\alpha_i}\rangle = \operatorname{Tr}_{\mathbb{A}}[\rho_{\mathbb{A}}\otimes_{i\in\mathbb{A}}A_i^{\alpha_i}]$. In [20] the density matrix $\tau_{\mathbb{A}}$ for cumulants was introduced, which makes it possible to estimate any cumulant $\langle\langle\otimes_{i\in\mathbb{A}}A_i^{\alpha_i}\rangle\rangle$ similarly:

$$\left\langle\left\langle \bigotimes_{i\in\mathbb{A}}A_i^{\alpha_i}\right\rangle\right\rangle = \operatorname{Tr}_{\mathbb{A}}\left[\tau_{\mathbb{A}}\bigotimes_{i\in\mathbb{A}}A_i^{\alpha_i}\right].$$
$$(24)$$

Also, it was shown that there is a relationship between the density matrix for cumulants and the common density matrix, which is similar to (23):

$$\tau_{\mathbb{A}} := \sum_{\pi\in\pi_{\mathbb{A}}}(|\pi|-1)!(-1)^{|\pi|-1}\bigotimes_{\mathbb{B}\in\pi}\rho_{\mathbb{B}}.$$
$$(25)$$

For example, the relation between density matrices for cumulants and the common density matrices for a subensemble of particles $\{1,2,3\}$ is similar to (22):

$$\tau_{\{1\}} = \rho_{\{1\}},$$

$$\tau_{\{1,2\}} = \rho_{\{1,2\}} - \rho_{\{1\}}\otimes\rho_{\{2\}},$$

$$\tau_{\{1,2,3\}} = \rho_{\{1,2,3\}} - \rho_{\{1,2\}}\otimes\rho_{\{3\}}$$
$$- \rho_{\{1,3\}}\otimes\rho_{\{2\}} - \rho_{\{1\}}\otimes\rho_{\{2,3\}} + 2\rho_{\{1\}}\otimes\rho_{\{2\}}\otimes\rho_{\{3\}}.$$

This relationship can also be written in the opposite direction, expressing the density matrices in terms of the density matrices for cumulants:

$$\rho_{\mathbb{A}} = \sum_{\pi\in\pi_{\mathbb{A}}}\bigotimes_{\mathbb{B}\in\pi}\tau_{\mathbb{B}},$$
$$(26)$$

wherefrom for the subensemble of particles $\{1,2,3\}$ it follows:

$$\rho_{\{1\}} = \tau_{\{1\}},$$

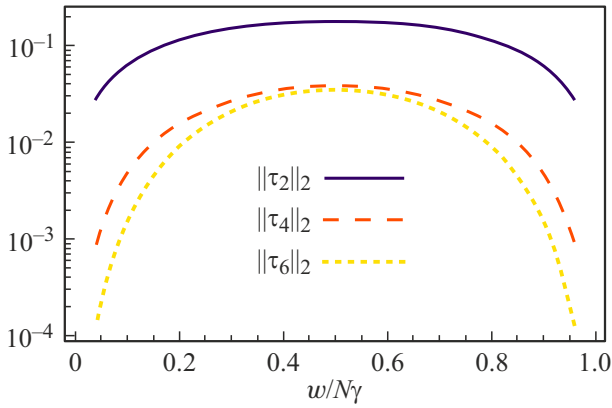$$\rho_{\{1,2\}} = \tau_{\{1,2\}} + \tau_{\{1\}}\otimes\tau_{\{2\}},$$

Figure 7. The Frobenius norm of the density matrix for τ_n cumulants vs. dimensionless pumping rate $w/N\gamma$. Number of atoms $N = 10^6$.

$$\rho_{\{1,2,3\}} = \tau_{\{1,2,3\}} + \tau_{\{1,2\}} \otimes \tau_{\{3\}} + \tau_{\{1,3\}} \otimes \tau_{\{2\}}$$
$$+ \tau_{\{1\}} \otimes \tau_{\{2,3\}} + \tau_{\{1\}} \otimes \tau_{\{2\}} \otimes \tau_{\{3\}}. \qquad (27)$$

Let us return to the master equation for the subensemble of n particles (21). Employing the relationship between the common density matrices and density matrices for cumulants, we write the truncated density matrix $\rho_{n+1}^{\text{trunc}}$ for $(n+1)$ particle: $\rho_{n+1}^{\text{trunc}} = \rho_{n+1} - \tau_{n+1}$. We subtracted the density matrix for cumulants τ_{n+1} from ρ_{n+1}, thereby removing information about the $(n+1)$th order correlations between $(n+1)$ particle from ρ_{n+1}. This allows to express $\rho_{n+1}^{\text{trunc}}$ as a function of ρ_n. For example, for the subensemble of three particles $\{1, 2, 3\}$ we have:

$$\rho_{\{1,2,3\}}^{\text{trunc}} = \tau_{\{1,2\}} \otimes \tau_{\{3\}} + \tau_{\{1,3\}} \otimes \tau_{\{2\}} + \tau_{\{1\}} \otimes \tau_{\{2,3\}}$$
$$+ \tau_{\{1\}} \otimes \tau_{\{2\}} \otimes \tau_{\{3\}} = \rho_{\{1,2\}} \otimes \rho_{\{3\}} + \rho_{\{1,3\}} \otimes \rho_{\{2\}}$$
$$+ \rho_{\{1\}} \otimes \rho_{\{2,3\}} - 2\rho_{\{1\}} \otimes \rho_{\{2\}} \otimes \rho_{\{3\}}, \qquad (28)$$

where we used (27). It can be seen that in the resulting expression, the right-hand side now depends on the lower-order density matrices, i.e. fewer particles. Thus, in (21), acting similarly, one can replace $\rho_{(n+1)}$ with $\rho_{(n+1)}^{\text{trunc}}$, which is a non-linear function of ρ_n, i.e., $\rho_{(n+1)}^{\text{trunc}} = f(\rho_n)$. As a result, we close the master equation for subensemble of n particles:

$$\dot{\rho}_n = L_n(\rho_n)$$
$$- \frac{1}{2}\gamma(N-n)\sum_{i=1}^{n}\left\{\sigma_-^{(i)}\text{Tr}_{\{n+1\}}[\sigma_+^{(n+1)}f(\rho_n)] + h.c.\right\}. \qquad (29)$$

This equation contains information about correlations in the system up to the nth order. Its stationary solution gives the density matrices for τ_n cumulants up to the nth order. Thus, the presence of a nonzero Frobenius norm at τ_n indicates the presence of the n-th order correlations in the system, i.e. correlations between n particles at once.

Fig. 7 shows the Frobenius norm of the density matrix τ_n for cumulants vs. the dimensionless pumping rate $w/N\gamma$ for $n \in \{2, 4, 6\}$ plotted in a logarithmic scale. It can be seen that for two-atom correlations $n = 2$ (solid line) this dependence coincides with the dependence for $\langle\sigma_1^+\sigma_2^-\rangle$ shown in Fig. 2. In this case, the values for correlations between 4 particles at $n = 4$ (dashed line) and 6 particles at $n = 6$ (dotted line) turn out to be significantly smaller than for $n = 2$ at any values of $w/N\gamma$. Note that τ_2 includes not only two-atom correlations of the form $\langle\sigma_1^+\sigma_2^-\rangle$. However, this type of correlations makes the largest contribution to the Frobenius norm. It is noteworthy that there are no correlations of odd orders in the stationary state for $N \gg 1$, due to the presence of permutation symmetry. This also correct for the generalized model of the superradiant laser whose atomic system density matrix obeys (8).

5. Conclusion

We considered the generalized model of the superradiant Raman laser, in which we took into account competing cooperative and individual processes that occur in atoms with a complex multilevel energy structure when they interact with external light fields. Using the projector method, we succeeded in adiabatically eliminating the rapidly decaying cavity mode and write the master equation for the density matrix describing the state of the atomic ensemble only. With its help, we found stationary solutions for the mean polarization (populations inversion) $\langle\sigma_1^z\rangle$ and two-atom correlations $\langle\sigma_1^+\sigma_2^-\rangle$, and after their analysis we estimated the threshold conditions for superradiance emission. Then, returning to the equation for the density matrix of the complete system, applying the quantum regression theorem, we calculated the two-time correlation function $\langle\hat{a}^\dagger(t)\hat{a}(0)\rangle$. Taking its Fourier transform we found the radiation spectrum $S(w)$. As we saw, the radiation spectrum contains two narrow Lorentz peaks, associated with competitive cooperative processes. The linewidth of these peaks turned out to be comparable with the effective decay rate of one atom γ_-. We also estimated the presence of high-order interatomic correlations by calculating the Frobenius norm of the density matrix for cumulants and showed that two-atom correlations make the largest contribution to stationary light generation.

The considered model can be used not only to estimate the properties of the superradiant laser, but also to study spin-polarized ensembles of alkali atoms with high optical density, which are continuously pumped and probed by external fields [21,22]. Such systems are of interest for numerous applications in quantum metrology and quantum information processing. As in the case when the atoms are inside the cavity, the high optical density in the direction of the optical axis creates a preferred direction in the medium, along which, due to the Purcell effect, the cooperative radiation of the ensemble occurs. This makes possible to introduce a „virtual" cavity and consider the ensemble

of atoms in the same way as the superradiant laser, i.e., employ the same methods as discussed in this paper. Thus, the obtained results can serve as a helpful reference for explanation of the occurring cooperative effects.

Acknowledgments

Funding

Conflict of interest

The authors declare that they have no conflict of interest.

References

[1] F. Haake, M.I. Kolobov, C. Fabre, E. Giacobino, S. Reynaud. Phys. Rev. Lett., **71**, 995 (1993). DOI: 10.1103/PhysRevLett.71.995

[2] R.H. Dicke. Phys. Rev., **93**, 99 (1954). DOI: 10.1103/PhysRev.93.99

[3] J.G. Bohnet, Z. Chen, J.M. Weiner, K.C. Cox, D. Meiser, M.J. Holland, J.K. Thompson. EPJ Web of Conferences, **57**, 03003 (2013). DOI: 10.1103/PhysRev.93.99

[4] D. Meiser, Jun Ye, D.R. Carlson, M.J. Holland. Phys. Rev. Lett., **102**, 163601 (2009). DOI: 10.1103/PhysRevLett.102.163601

[5] B.C. Young, F.C. Cruz, W.M. Itano, J.C. Bergquist. Phys. Rev. Lett., **82**, 3799 (1999). DOI: 10.1103/PhysRevLett.82.3799

[6] S.A. Webster, M. Oxborrow, P. Gill. Phys. Rev. A, **75**, 011801(R) (2007). DOI: 10.1103/PhysRevA.75.011801

[7] J.A. Muniz , J.R.K. Cline, M.A. Norcia, J.K. Thompson. In: *Proc. SPIE 10934, Optical, Opto-Atomic, and Entanglement-Enhanced Precision Metrology*, v. 109342B (SPIE Digital Library, 2019). DOI 10.1117/12.2515582

[8] J.G. Bohnet, Z. Chen, J.M. Weiner, D. Meiser, M.J. Holland, J.K. Thompson. Nature **484**, 78?81 (2012). DOI 10.1038/nature10920

[9] J.M. Weiner, K.C. Cox, J.G. Bohnet, J.K. Thompson. Phys. Rev. A, **95**, 033808 (2017). DOI: 10.1103/PhysRevA.95.033808

[10] J.M. Weiner, K.C. Cox, J.G. Bohnet, Z. Chen, J.K. Thompson. Appl. Phys. Lett., **101**, 261107 (2012). DOI: 10.1063/1.4773241

[11] G.S. Agarwal. Phys. Rev. A, **83**, 023802 (2011). DOI: 10.1103/PhysRevA.83.023802

[12] D. Meiser, M.J. Holland. Phys. Rev. A, **81**, 063827 (2010). DOI: 10.1103/PhysRevA.81.063827

[13] F. Haake, M.I. Kolobov, C. Seeger, C. Fabre, E. Giacobino, S. Reynaud. Phys. Rev. A, **54**, 1625 (1996). DOI: 10.1103/PhysRevA.54.1625

[14] C.W. Gardiner, P. Zoller. *Quantum noise: a handbook of Markovian and non-Markovian quantum stochastic methods with applications to quantum optics*, 3rd ed. (Springer Berlin, Heidelberg, 2004).

[15] M. Xu, D.A. Tieri, E.C. Fine, J.K. Thompson, M.J. Holland, Phys. Rev. Lett., **113**, 154101 (2014). DOI: 10.1103/PhysRevLett.113.154101

[16] A.P. Kazantsev, G.I. Surdutovich, V.P. Yakovlev. *Mechanical Action of Light on Atoms* (World Scientific Publishing, Singapore, 1990). DOI: 10.1142/0585.

[17] A.A. Budini, J. Stat. Phys., **131**, 51 (2008). DOI: 10.1007/s10955-007-9476-9

[18] A.S. Chirkin, O.V. Belyaeva, A.V. Belinsky. J. Exp. Theor. Phys., **116** (1), 39 (2013). DOI 10.1134/S1063776113010202

[19] A.N. Malakhov. *Kumulyantny analiz sluchajnykh negaussovykh protsessov i ikh preobrazovaniy* (Sovetskoe radio, Moscow, 1978 (in Russian)

[20] A. Roth. *Collective effects and superradiance in atomic ensembles*. PhD Thesis (Leibniz University Hannover, Hannover, 2018). DOI: 10.15488/3856

[21] A.S. Parkins, E. Solano, J.I. Cirac. Phys. Rev. Lett., **96**, 053602 (2006). DOI: 10.1103/PhysRevLett.96.053602

[22] C.A. Muschik, E.S. Polzik, J.I. Cirac. Phys. Rev. A, **83**, 052312 (2011). DOI: 10.1103/PhysRevA.83.052312